AIP | Physics of Fluids

Dispersion due to electroosmotic flow in a circular microchannel with slowly varying wall potential and hydrodynamic slippage

Chiu-On Ng and Qi Zhou

Citation: Phys. Fluids **24**, 112002 (2012); doi: 10.1063/1.4766598
View online: http://dx.doi.org/10.1063/1.4766598
View Table of Contents: http://pof.aip.org/resource/1/PHFLE6/v24/i11
Published by the American Institute of Physics.

Dispersion due to electroosmotic flow in a circular microchannel with slowly varying wall potential and hydrodynamic slippage

Chiu-On Ng[a] and Qi Zhou
Department of Mechanical Engineering, The University of Hong Kong, Pokfulam Road, Hong Kong

(Received 18 April 2012; accepted 23 October 2012; published online 12 November 2012)

An analysis using the lubrication approximation is performed for the dispersion of a neutral non-reacting solute due to electro-osmotic flow through a circular channel under the combined effects of longitudinal non-uniformity of potential and hydrodynamic slippage on the channel wall. The wall is periodically patterned for the charge and slip distributions, with a wavelength much longer than the channel radius. It is shown that the presence of slip can greatly amplify the increased dispersion caused by induced pressure gradient brought about by the non-uniformity of wall potential. Non-uniform wall potential interacting with non-uniform slip can give rise to effects much different from those when the potential and slip are both uniformly distributed and equal to the averages of the non-uniform distributions. Mobility and dispersion associated with recirculating flow resulting from oppositely charged slipping region is also examined. © *2012 American Institute of Physics*. [http://dx.doi.org/10.1063/1.4766598]

I. INTRODUCTION

Mixing and separation of chemical species are two major fluidic processes to be performed in a lab-on-a-chip or micro-total-analysis system. The two problems of mixing and separation are opposite to each other in terms of operating conditions for the mass transport. While mechanisms like diffusion and dispersion are desirable in the case of mixing, they are unwanted in the case of separation. In microfluidics, increasing the efficiency of either the mixing or separation is not a trivial matter.[1] Dispersion or band broadening will limit the performance of chemical analysis systems such as capillary zone electrophoresis and capillary liquid chromatography with electro-osmotic flow. This has motivated many studies to investigate dispersion in flow driven by electrokinetics.

The electrokinetic method viz. electroosmosis (EO), which mobilizes fluid utilizing the unbalanced charge density in an electric double layer (EDL), has now been widely applied to microfluidics as it offers the ability to control and drive fluid by external means without mechanical moving parts. The application of an electric field, together with the electric double layer formed at the contact interface of an electrolyte and a solid surface, gives rise to electro-osmotic flow (EOF), which is in several aspects superior to pressure-driven flow.

Compared with transport in pressure-driven (Poiseuille) flow, electro-osmotic flow under the condition of a thin EDL may generate much weaker hydrodynamic dispersion. This is because when the EDL is thin, the electro-osmotic flow has an essentially flat profile, which, in the absence of any velocity shear, produces negligible dispersion. In sharp contrast, Poiseuille flow has a parabolic profile, which may produce significant dispersion if the velocity (more precisely, the Péclet number) is sufficiently large. This fundamental difference has made EO a better choice of driving mechanism when transport with limited dispersion is wanted.

[a] Author to whom correspondence should be addressed. Electronic mail: cong@hku.hk.

One of the earliest theoretical studies on dispersion in EO flow is due to Martin and Guiochon,[2] who analyzed zone broadening resulting from EO flow and retention in open-tubular capillary liquid chromatography. Their analysis was, however, based on an approximated EO velocity profile. Electrokinetic dispersion in circular capillary electrophoresis without adsorption was then studied by Datta and Kotamarthi,[3] accounting for the combined effects of Poiseuille and EO flows for the case of low wall potential (also known as zeta potential). Griffiths and Nilson[4] analytically determined the dispersion in EO flow, for both a circular tube and a parallel-plate channel, by solving the time-dependent diffusion-advection equation in transformed coordinates, where the dispersion coefficient arises as an eigenvalue satisfying the boundary conditions. For zeta potentials not necessarily small, these authors[5] numerically computed the dispersion coefficient over a broad range of the EDL thickness and the zeta potential. Zholkovskij *et al.*[6] and Zholkovskij and Masliyah[7] further examined, under the condition of a thin EDL and hence using the Smoluchowski approximation, hydrodynamic dispersion due to purely EOF or combined (pressure-driven and EO) flow for arbitrary potential, electrolyte type, and cross-section geometry.

All these above-mentioned works are based on the assumption that the capillary surface is homogeneous carrying a uniform charge density, and hence the flow is essentially unidirectional. Wall heterogeneity, which may occur either naturally or artificially by construction, can lead to opposite effects on the dispersion depending on whether the flow is driven by pressure or electric field. Dispersion is reduced for pressure-driven flow, but is increased for EO flow, when there are heterogeneities on the channel walls. It is because surface non-uniformity, such as surface topography[8] or opposite charges on opposing walls,[9] can generate transverse or secondary flow, which enhances mixing in the cross section, and will therefore reduce dispersion in the case of pressure-driven flow. Meanwhile, surface non-uniformity also leads to an induced pressure gradient, which is required in order to maintain the flow continuity. When this happens to an EO flow, the plug-like uniform velocity profile will be contaminated by the parabolic velocity profile of the induced pressure-driven flow. This explains why dispersion can be increased by surface non-uniformity in the case of EO flow. This undesirable effect due to surface heterogeneity on dispersion in EO flow has been studied in the context of electrokinetic chromatography or electrophoretic separation, as noted below.

Through numerical simulations, Potoček *et al.*[10] showed that the plug-like EO flow cannot be materialized when the zeta potential is longitudinally inhomogeneous, which may lead to significant dispersion of sample peaks. Effects of flow perturbations due to surface defects on dispersion in capillary electrophoresis were analytically examined by Long *et al.*[11] Pressure jump is induced by the presence of surface defects, resulting in possible occurrence of recirculating flows. They showed that a single defect, from which the velocity perturbation decays only algebraically, can cause hydrodynamic dispersion over a large distance. The same problem was investigated analytically and experimentally by Herr *et al.*,[12] who considered discrete step change in the zeta potential (from EOF supporting to EOF suppressing) introduced at various distances along the length of a cylindrical capillary. They provided empirical evidence showing that the dispersion in the EOF-supporting region increases as the percentage of the EOF-suppressing length increases. The theory of Herr *et al.*[12] was applied by Ghosal[13] to compare with the experiments by Towns and Regnier,[14] in an attempt to show that decreased resolution in capillary zone electrophoresis is caused by dispersion arising from pressure gradient brought about by the non-uniformity of wall potential. Ghosal[15] also presented an asymptotic theory for the electrophoretic transport of species when the wall potential is locally modified by adsorption of the species onto the wall from the fluid stream. More recently, Zholkovskij *et al.*[16] studied band broadening of a neutral solute in EO flow through a submicrometer channel with longitudinal non-uniformity of zeta potential. Their model is more general in the sense that it is applicable to arbitrary cross-section geometry, electrolyte composition and potential.

All the existing studies on electrically driven hydrodynamic dispersion is based on flow subject to the no-slip boundary condition on the capillary surface. In microchannels, such a boundary condition may not be valid. The channel wall can be engineered to form a stick–slip micro-pattern, or chemically treated to become hydrophobic, resulting in a low-viscosity or depletion layer lubricating the flow over the surface, amounting to boundary slip. It has been well known that even a small amount of boundary slippage can substantially enhance electro-osmotic flow, since the first analysis

by Muller *et al.*[17] In the thin EDL limit, the EOF is enhanced by a factor equal to the ratio of the effective slip length to the Debye length (the thickness of the EDL). Such a linear factor of EOF enhancement due to boundary slip was proposed by Churaev *et al.*[18] and verified with molecular dynamics simulations by Joly *et al.*[19] By this factor, slip lengths in the nano- to micrometer range can result in a very large enhancement, as much as two orders of magnitude, owing to the much thinner electric double layer.[20]

Since EO flow can be sensitively affected by hydrodynamic slip, it is of interest to study how dispersion in EO flow can be affected by slip. No such study exists in the literature, however. This has motivated the present problem, which aims to look into dispersion arising from electrically driven flow in a circular microchannel with longitudinal non-uniformity of both wall potential and hydrodynamic slippage. It is our objective here to demonstrate how the presence of slip may dramatically change the effect of non-uniform wall potential on the dispersion. Non-uniform wall potential interacting with non-uniform slip can lead to effects more intensive than those when the wall potential and slip are both uniform and equal to the system averages of the non-uniform distributions. EO flow through a channel with inhomogeneously charged superhydrophobic surfaces has been recently investigated by Squires,[21] Bahga *et al.*,[22] Zhao,[23] Vinogradova and Belyaev,[24] Belyaev and Vinogradova,[25] and Ng and Chu.[26] Solute transport is, however, not covered in these studies. Belyaev and Vinogradova[25] showed that it is possible to form convective rolls when the slipping region is oppositely charged; such recirculating flow is conducive to mixing. In the present study, the dispersion associated with recirculating flow over an oppositely charged slipping surface is examined in particular.

Our problem is described in further detail in Sec. II, where we derive expressions for electro-osmotic flow through a circular microchannel with axial variations in both wall potential and hydrodynamic slip length. The electric double layer is of arbitrary thickness as long as it is not strongly overlapped at the center of the channel. The slip length is of the same length scale as the channel radius, which is much smaller than the length scale for variations of wall charge and slip along the axis of the channel. The sharp contrast in length scales enables the application of the lubrication theory to the present problem. For electrokinetic flow problems, the lubrication approximation has been applied previously by Ajdari,[27,28] Long *et al.*,[11] Ghosal,[15,29] and Ng and Zhou.[30] We shall then derive in Sec. III an expression for the hydrodynamic dispersion coefficient arising from the flow. It is shown that the coefficient, which appears to have essentially the same formal expression as that for flow in a no-slip channel, is subject to the combined effect of non-uniform charge and slip distributions through the induced pressure gradient. Results are then discussed in Sec. IV, where we examine in some detail the effects of non-uniform wall potential, when interacting with boundary slip, on the system average as well as the axial distribution of the dispersion coefficient. We shall identify various scenarios corresponding to high/low EO mobility with strong/weak dispersion.

II. FLOW

We consider hydrodynamic dispersion of a neutral non-reacting species in steady EO flow through a circular channel, on the wall of which the electro-hydrodynamic properties vary gradually and periodically with axial position. The zeta or wall potential ζ and the hydrodynamic slip length δ are periodic functions of the axial coordinate z, where the wavelength of one periodic unit L, which is the length scale for variations in the axial direction, is much longer than the channel radius R, which is the length scale for variations in the radial direction. The sharp contrast in length scales, i.e., $\varepsilon \equiv R/L \ll 1$, implies that the rate of change is much slower in the axial direction than in the radial direction. We further assume that the Reynolds number Re of the flow is such that $\varepsilon\mathrm{Re} \ll 1$, by which the inertial terms are much smaller than the leading viscous diffusion term. These two conditions of smallness, one geometric and one dynamic, are the basic requirements for the lubrication approximation.[31] Under these conditions, the inertia is negligible and the flow is nearly one-dimensional; the radial velocity is an order smaller than the axial velocity. Also, the pressure is locally uniform across the channel, and derivatives with respect to the axial coordinate z are subdominant compared with those with respect to the radial coordinate r. Axisymmetric flow is assumed.

For sufficiently low zeta potential ($\ll$25 mV) and a non-overlapped EDL, the linearized Poisson–Boltzmann equation for the electric potential $\psi(r, z)$ of a symmetric binary electrolyte reads in the lubrication approximation as follows:

$$\frac{1}{r}\frac{\partial}{\partial r}\left(r\frac{\partial \psi}{\partial r}\right) = \kappa^2 \psi, \tag{1}$$

where κ is the Debye–Hückel parameter, or the inverse of the Debye length (a measure of the thickness of the EDL). Subject to the boundary conditions: $\psi = \zeta(z)$ at the wall $r = R$, and ψ is finite at the center $r = 0$, the potential can be readily found to be

$$\psi(r, z) = \zeta(z)\frac{I_0(\kappa r)}{I_0(\kappa R)}, \tag{2}$$

where I_n is the modified Bessel function of the first kind of order n. The solution is valid for any distribution of the zeta potential $\zeta(z)$ that is a slow function of z, as long as the potential remains smaller than 25 mV at room temperature. We leave the function unspecified for the time being.

Flow is driven by an applied electric field E_z in the z-direction. There are no externally applied pressure gradients. Pressure is, however, locally induced in order to maintain continuity of flow. In the lubrication limit, the flow is nearly unidirectional along the axis of the channel. The approximate z-momentum equation reads

$$\frac{1}{r}\frac{\partial}{\partial r}\left(r\frac{\partial u}{\partial r}\right) = \frac{1}{\mu}\frac{\partial p'}{\partial z} + \frac{\epsilon\kappa^2 E_z}{\mu}\psi, \tag{3}$$

where $u(r, z)$ is the z-component velocity, μ is the fluid dynamic viscosity, ϵ is the dielectric constant of the electrolyte, and $p'(z) = p - \epsilon\kappa^2\psi^2/2$ is the effective pressure (the electrostatic pressure being subtracted from the pressure p).

The flow is subject to a first-order partial-slip condition at the wall

$$u + \delta\frac{\partial u}{\partial r} = 0 \qquad \text{at } r = R, \tag{4}$$

where $\delta(z)$ is the local hydrodynamic slip length, which can be any slow function of z. We also leave it unspecified for the time being. Slip length can be interpreted as the distance into the wall where the velocity profile extrapolates to zero.

The axial velocity satisfying the slip condition at the wall and the condition of zero stress at the center is

$$u(r, z) = -\frac{R^2}{4\mu}\frac{\partial p'}{\partial z}\left(1 - \frac{r^2}{R^2} + \frac{2\delta}{R}\right) - \frac{\epsilon E_z}{\mu}\zeta\left[1 - \frac{I_0(\kappa r)}{I_0(\kappa R)} + \kappa\delta\frac{I_1(\kappa R)}{I_0(\kappa R)}\right], \tag{5}$$

which, in the case of zero slip, agrees with the one deduced by Rice and Whitehead.[32] We introduce the following normalized variables (distinguished by an overhead caret):

$$\hat{z} = z/L, \quad (\hat{r}, \hat{\delta}) = (r, \delta)/R, \quad \hat{\kappa} = \kappa R, \quad \hat{\zeta} = \zeta/\zeta_0, \tag{6}$$

where L is the wavelength of the wall pattern, R is the channel radius, and $\zeta_0 = k_B T/(z_0 e)$ (k_B is the Boltzmann constant, T is the absolute temperature, z_0 is the valence of the electrolyte, e is the elementary charge) is a scale for the wall potential, which should be of a magnitude much smaller than 25 mV at room temperature for a binary electrolyte. On averaging across the section, the section-mean EO velocity is given by

$$\bar{u} = 2\int_0^1 \hat{r}u d\hat{r} = A(\hat{z})U_{\mathrm{PO}}(\hat{z}) + B(\hat{z})U_{\mathrm{EO}}, \tag{7}$$

where

$$U_{\mathrm{PO}}(\hat{z}) = -\frac{R^2}{8\mu}\frac{\partial p'}{\partial z}, \qquad U_{\mathrm{EO}} = -\frac{\epsilon\zeta_0}{\mu}E_z \tag{8}$$

are forcings terms with dimensions of velocity, and

$$A(\hat{z}) = 1 + 4\hat{\delta}(\hat{z}), \tag{9}$$

$$B(\hat{z}) = \hat{\zeta}(\hat{z})\left[1 + \left(\hat{\kappa}\hat{\delta}(\hat{z}) - \frac{2}{\hat{\kappa}}\right)\frac{I_1(\hat{\kappa})}{I_0(\hat{\kappa})}\right]. \tag{10}$$

The term U_{PO} is equivalent to the mean velocity of Poiseuille flow in a no-slip circular tube, while U_{EO} is the Helmholtz–Smoluchowski velocity of EO flow.

By continuity, the section-mean velocity $\bar{u}$ is independent of the axial coordinate $\hat{z}$. On rearranging Eq. (7),

$$U_{\mathrm{PO}}(\hat{z}) = \frac{\bar{u}}{A(\hat{z})} - \frac{B(\hat{z})}{A(\hat{z})}U_{\mathrm{EO}}. \tag{11}$$

We here introduce angle brackets to denote averaging over one wavelength along the channel. For any function $f(\hat{z})$, the average along the length of channel is given by

$$\langle f \rangle \equiv \int_0^1 f d\hat{z}. \tag{12}$$

We consider the flow to be induced without an externally applied pressure gradient. Therefore, the pressure drop across one periodic unit is zero, or $\langle U_{\mathrm{PO}} \rangle = 0$, by which the axial averaging of Eq. (11) gives

$$0 = \bar{u}\left\langle \frac{1}{A(\hat{z})} \right\rangle - \left\langle \frac{B(\hat{z})}{A(\hat{z})} \right\rangle U_{\mathrm{EO}} \tag{13}$$

or

$$\bar{u} = MU_{\mathrm{EO}}, \tag{14}$$

where

$$M = \frac{\langle B(\hat{z})/A(\hat{z}) \rangle}{\langle 1/A(\hat{z}) \rangle} \tag{15}$$

is the EO mobility. Putting Eq. (14) back to Eq. (11), the induced pressure gradient is

$$U_{\mathrm{PO}}(\hat{z}) = G(\hat{z})U_{\mathrm{EO}}, \tag{16}$$

where the dimensionless function

$$G(\hat{z}) = \frac{M - B(\hat{z})}{A(\hat{z})} \tag{17}$$

can be interpreted as the ratio of the induced hydrodynamic forcing to the applied electrokinetic forcing. The velocity in Eq. (5) can now be written in a dimensionless form as

$$\hat{u}(\hat{r}, \hat{z}) = u/U_{\mathrm{EO}} = 2G(\hat{z})\left(1 + 2\hat{\delta}(\hat{z}) - \hat{r}^2\right) + \hat{\zeta}(\hat{z})\left[F(\hat{z}) - \frac{I_0(\hat{\kappa}\hat{r})}{I_0(\hat{\kappa})}\right], \tag{18}$$

where

$$F(\hat{z}) = 1 + \hat{\kappa}\hat{\delta}(\hat{z})\frac{I_1(\hat{\kappa})}{I_0(\hat{\kappa})}. \tag{19}$$

The dimensionless streamfunction is then given by

$$\Psi(\hat{r}, \hat{z}) = \int_0^{\hat{r}} \hat{r}\hat{u}d\hat{r} = 2G(\hat{z})\left[\left(1 + 2\hat{\delta}(\hat{z})\right)\frac{\hat{r}^2}{2} - \frac{\hat{r}^4}{4}\right] + \hat{\zeta}(\hat{z})\left[F(\hat{z})\frac{\hat{r}^2}{2} - \frac{\hat{r}}{\hat{\kappa}}\frac{I_1(\hat{\kappa}\hat{r})}{I_0(\hat{\kappa})}\right]. \tag{20}$$

If we consider the flow to be driven instead by an applied pressure gradient K such that $\langle U_{\mathrm{PO}} \rangle = KR^2/\mu$, the effective hydrodynamic slip length can be deduced from Eq. (11) as

$$\hat{\delta}_{\mathrm{eff}} = \frac{1}{4}\left\langle \frac{1}{A(\hat{z})} \right\rangle^{-1} - \frac{1}{4}. \tag{21}$$

We now consider two particular cases. First, for uniformly distributed slip length, i.e., $\hat{\delta} = \hat{\delta}_{\mathrm{const}}$ = constant, the effective slip length can be checked to be simply equal to the constant slip length

$\hat{\delta}_{\text{eff}} = \hat{\delta}_{\text{const}}$, and the section-mean EO velocity is then given by

$$\bar{u} = \langle B \rangle U_{\text{EO}} = \langle \hat{\zeta} \rangle \left[1 + \left(\hat{\kappa} \hat{\delta}_{\text{const}} - \frac{2}{\hat{\kappa}} \right) \frac{I_1(\hat{\kappa})}{I_0(\hat{\kappa})} \right] U_{\text{EO}} \qquad \text{for constant } \hat{\delta}, \tag{22}$$

which agrees with the steady-state limit deduced by Yang and Kwok,[33] who studied oscillating EO flow in circular channels under the effect of hydrodynamic slippage. Second, for uniformly distributed wall potential such that $\hat{\zeta} = \hat{\zeta}_{\text{const}} =$ constant, the section-mean EO velocity can be found to be

$$\bar{u} = \hat{\zeta}_{\text{const}} \left[1 + \left(\hat{\kappa} \hat{\delta}_{\text{eff}} - \frac{2}{\hat{\kappa}} \right) \frac{I_1(\hat{\kappa})}{I_0(\hat{\kappa})} \right] U_{\text{EO}} \qquad \text{for constant } \hat{\zeta}. \tag{23}$$

This is a result reminiscent of a previous finding by Squires.[21] In the limit of a very thin EDL $\hat{\kappa} \to \infty$, by which $\hat{\kappa}^{-1} \to 0$ and the ratio of the two modified Bessel functions $I_1(\hat{\kappa})/I_0(\hat{\kappa}) \to 1$, Eq. (23) reduces to

$$\lim_{\hat{\kappa} \to \infty} \bar{u} = \hat{\zeta}_{\text{const}} \left[1 + \hat{\kappa} \hat{\delta}_{\text{eff}} \right] U_{\text{EO}}, \tag{24}$$

which is identical in form to the expression for EO velocity deduced by Squires.[21] His finding is as follows. For flow over a heterogeneous plane surface (i.e., very thick channel) under the condition of a very thin EDL, Squires theoretically showed that when the wall is uniformly charged, the effective EO velocity is given by exactly the same expression as would be obtained by naïvely assuming homogeneous slip with a slip length equal to the effective slip length of the heterogeneous surface. We have formally proved that this statement will remain true even when the channel is of finite thickness and the EDL is not necessarily very thin,[26] or even when the flow is oscillatory.[34] Here, we may infer from Eqs. (22) and (23) that Squires' statement is also applicable to EO flow through a circular channel where the EDL is not necessarily very thin.

III. HYDRODYNAMIC DISPERSION

The dispersion coefficient controls the rate of spreading of a solute cloud about its center of distribution. In the present problem, as a result of the velocity profile changing axially, the dispersion coefficient is a function of axial position. In the lubrication limit, we may, however, assume that the dispersion coefficient depends on the axial coordinate only parametrically. It is formally given by the same expression as the one for strictly unidirectional flow. The long-time fully developed or steady-state dispersion coefficient D_T, also known as the Taylor dispersion coefficient, is given by (e.g., Mei *et al.*,[35] Ng[36])

$$D_T = \bar{N} \bar{u} - \overline{Nu}, \tag{25}$$

where the overhead bar denotes averaging across the section, and the function $N(r)$ is governed by

$$\frac{D}{r} \frac{d}{dr} \left(r \frac{dN}{dr} \right) = u - \bar{u}, \qquad \text{in } 0 < r < R, \tag{26}$$

where D is the molecular diffusivity. The equation above is subject to the boundary conditions that N is finite at $r = 0$ and $dN/dr = 0$ at $r = R$.

Substituting Eqs. (14) and (18) for u and $\bar{u}$, we may readily solve Eq. (26) for $N(\hat{r})$ to get

$$\left(\frac{D}{R^2 U_{\text{EO}}} \right) N(\hat{r}) = 2G \left[\left(1 + 2\hat{\delta} \right) \frac{\hat{r}^2}{4} - \frac{\hat{r}^4}{16} \right] + \hat{\zeta} \left[F \frac{\hat{r}^2}{4} - \frac{I_0(\hat{\kappa}\hat{r})}{\hat{\kappa}^2 I_0(\hat{\kappa})} \right] - M \frac{\hat{r}^2}{4}. \tag{27}$$

On putting this into Eq. (25), and after some lengthy but straightforward algebra, the following expression for the dispersion coefficient can be obtained:

$$D_T = \left\{ X_p G^2(\hat{z}) + X_{pe} G(\hat{z}) \hat{\zeta}(\hat{z}) + X_e \hat{\zeta}^2(\hat{z}) \right\} \frac{R^2 U_{\text{EO}}^2}{D}, \tag{28}$$

where

$$X_p = \frac{1}{48}, \tag{29}$$

$$X_{pe}(\hat{\kappa}) = \left(\frac{1}{6\hat{\kappa}} - \frac{4}{\hat{\kappa}^3} - \frac{32}{\hat{\kappa}^5}\right)\frac{I_1(\hat{\kappa})}{I_0(\hat{\kappa})} + \frac{16}{\hat{\kappa}^4}, \tag{30}$$

$$X_e(\hat{\kappa}) = \left(\frac{3}{2\hat{\kappa}^2} + \frac{8}{\hat{\kappa}^4}\right)\frac{I_1^2(\hat{\kappa})}{I_0^2(\hat{\kappa})} - \frac{2}{\hat{\kappa}^3}\frac{I_1(\hat{\kappa})}{I_0(\hat{\kappa})} - \frac{1}{\hat{\kappa}^2}. \tag{31}$$

The total diffusion constant (also known as the Taylor–Aris dispersion coefficient) is the sum of the molecular diffusivity and the Taylor dispersion coefficient

$$D_{\text{eff}} = D + D_T = D\left(1 + \hat{D}_T \text{Pe}^2\right), \tag{32}$$

where $\hat{D}_T = D_T/(R^2U_{\text{EO}}^2/D)$ is a normalized form of the dispersion coefficient, and $\text{Pe} = RU_{\text{EO}}/D$ is the Péclet number. Taylor dispersion will dominate over molecular diffusion when $\hat{D}_T\text{Pe}^2 \gg 1$.

The normalized dispersion coefficient $\hat{D}_T = X_pG^2 + X_{pe}G\hat{\zeta} + X_e\hat{\zeta}^2$ is to vary parametrically with axial position through the dependence on $\hat{z}$ of G and $\hat{\zeta}$. It is a function of the local values, as well as the system averages, of the slip and wall potential. Note that the three prefactors X_p, X_{pe}, and X_e are all independent of the slip length. Hence, the dispersion coefficient is affected by the slip only through the function G, which depends on the slip length $\hat{\delta}(\hat{z})$, as can be seen from Eqs. (9), (10), (15), and (17). Also note that G and $\hat{\zeta}$ are, respectively, the terms associated with the flows driven by the pressure gradient and electric field. Hence, the three components for the dispersion coefficient given in Eq. (28) are the components arising from the pressure-driven flow alone (as can be recognized by the well-known factor of 1/48), from the interaction between the pressure-driven and EO flows, and from the EO flow alone, respectively. These three components, with their prefactors given above, can be checked to match with those deduced by Datta and Kotamarthi.[3] For flows caused by independent forcings of pressure difference and electric field in a no-slip circular capillary with uniform surface charge density, Datta and Kotamarthi[3] derived an expression, also consisting of three components, for the dispersion coefficient accounting for the combined effects of hydrodynamic and electrokinetic flows. In our problem, the two forcings are not independent of each other (as the pressure is induced), and a heterogeneous wall with spatially varying slip and potential is considered. Despite these differences, we have under the lubrication approximation obtained an expression that is formally the same as theirs.

In the particular case when the wall is homogeneous so that both the wall potential and slip are uniformly distributed, $\hat{\delta}$ and $\hat{\zeta}$ are constants (say, $\hat{\zeta} = 1$), and $G = 0$ as no pressure needs to be induced. The dispersion coefficient then reduces to

$$\hat{D}_T = X_e \qquad \text{for constant } \hat{\delta} \text{ and } \hat{\zeta} = 1, \tag{33}$$

which is completely independent of $\hat{\delta}$, as expected. This limiting dispersion coefficient is the same as the one previously deduced by Griffiths and Nilson[4] for electrokinetic dispersion in a no-slip circular tube. As has been pointed out and shown by Ng,[37] the dispersion coefficient will not be affected by uniformly distributed slip. This is because the boundary slip, which is constant everywhere, is to shift uniformly the velocity profile, but will not change the velocity gradient, which determines the dispersion coefficient. Hence, in the particular case of a homogeneous wall, the slip is to enhance the flow, but will have no effect on the dispersion coefficient. One can analytically show that the function $X_e(\hat{\kappa})$ tends to zero at the two limits: $\hat{\kappa} \to 0$ and $\hat{\kappa} \to \infty$ (i.e., very thick and very thin EDL, respectively). Although beyond the bound of our theory, the limit $\hat{\kappa} \to 0$ is considered here only to demonstrate the trend of the physical phenomena. The two asymptotic limits are as follows. For a very thick EDL,

$$X_e \to \frac{\hat{\kappa}^4}{3072} \qquad \text{as } \hat{\kappa} \to 0, \tag{34}$$

which asymptotically tends to zero because the mean velocity decreases according to $\hat{\kappa}^2$ as $\hat{\kappa} \to 0$. As slip has no effect on dispersion in this particular case, the mean velocity that we are referring to is

$$\hat{\bar{u}}_0 = \lim_{\hat{\kappa}\to 0} \hat{\bar{u}}(\hat{\delta} = 0) = \hat{\kappa}^2/8, \tag{35}$$

as can be deduced from Eq. (23). Therefore, the limit Eq. (34) can also be written as $X_e \to \hat{\bar{u}}_0^2/48$ as $\hat{\kappa} \to 0$. In this limit, the EO flow has a parabolic profile, thereby leading to a dispersion coefficient that has the same numerical factor (1/48) as the one for pressure-driven flow.[4,5] In the other limit of a very thin EDL,

$$X_e \to \frac{1}{2\hat{\kappa}^2} \qquad \text{as } \hat{\kappa} \to \infty, \tag{36}$$

which asymptotically tends to zero because the EO flow is increasingly like a plug flow as $\hat{\kappa}$ increases. The numerical factor of 1/2 was also theoretically obtained by Zholkovskij *et al.*[6] for electro-osmotically driven dispersion in a no-slip circular channel with a thin EDL. This limiting value is practically achieved when $\hat{\kappa} > 10^3$. From Eq. (33) and the two limits above, one also finds that, as pointed out by Griffiths and Nilson,[4] the ratio of the dispersion coefficient to the molecular diffusion coefficient, D_T/D, is proportional to the square of the Péclet number as in Eq. (32), which is based on the channel radius R when $\hat{\kappa} \le O(1)$ (thick EDL), or based on the Debye length κ^{-1} itself when $\hat{\kappa} \gg 1$ (thin EDL). Furthermore, one can numerically show that the function $X_e(\hat{\kappa})$ reaches the maximum value of 0.00382775 when $\hat{\kappa} = 4.68$. The dispersion coefficient in Eq. (33) therefore has the peak value of

$$\max \hat{D}_T = 0.003828 \quad \text{at } \hat{\kappa} = 4.68, \text{ for constant } \hat{\delta} \text{ and } \hat{\zeta} = 1. \tag{37}$$

The Debye length is typically very small, $\hat{\kappa} \ge O(1)$, for which the dispersion coefficient is $\hat{D}_T \le O(10^{-3})$. The dispersion coefficient is indeed very small in this limiting case of a homogeneous wall. We shall show in Sec. IV that the dispersion coefficient can be enhanced by heterogeneities of the wall. Uniformly distributed wall slippage will have no effect on the dispersion coefficient when the wall potential is also uniformly distributed, but can have significant effect on the dispersion coefficient when the wall potential is non-uniformly distributed.

IV. DISCUSSION

Let us assume that the wall is sinusoidally modulated with the same wavelength for the slip length and the wall potential, as given below

$$\hat{\delta}(\hat{z}) = \hat{\delta}_0 \left[1 + \sigma \cos(2\pi \hat{z})\right], \tag{38}$$

$$\hat{\zeta}(\hat{z}) = a + b \cos(2\pi \hat{z}). \tag{39}$$

In these expressions, $\hat{\delta}_0$ and a are the system average values (i.e., the steady components) for the slip length and potential of the wall, respectively, and b is the amplitude of the alternating modulation component of the wall potential. The parameter σ is an integer equal to 1 or 0, corresponding to a non-uniform or uniform distribution of the slip length. For validity of the lubrication approximation, we require that $\hat{\delta}_0\sigma$ and b must not exceed order unity. Slip length may vary between the maximum value of $2\delta_0$ and the minimum value of zero. Negative slip length is not considered here. The wall potential, however, may be positive or negative (a positive/negative normalized potential $\hat{\zeta}$ means that the potential ζ is of the same/opposite sign as the reference potential ζ_0). A value of $\hat{\kappa} = 10$ for the Debye–Hückel parameter is used in all the cases discussed below. We compare the dispersion coefficient of different cases based on the spatially averaged dispersion coefficient

$$\langle \hat{D}_T \rangle = \int_0^1 \hat{D}_T \, d\hat{z}. \tag{40}$$

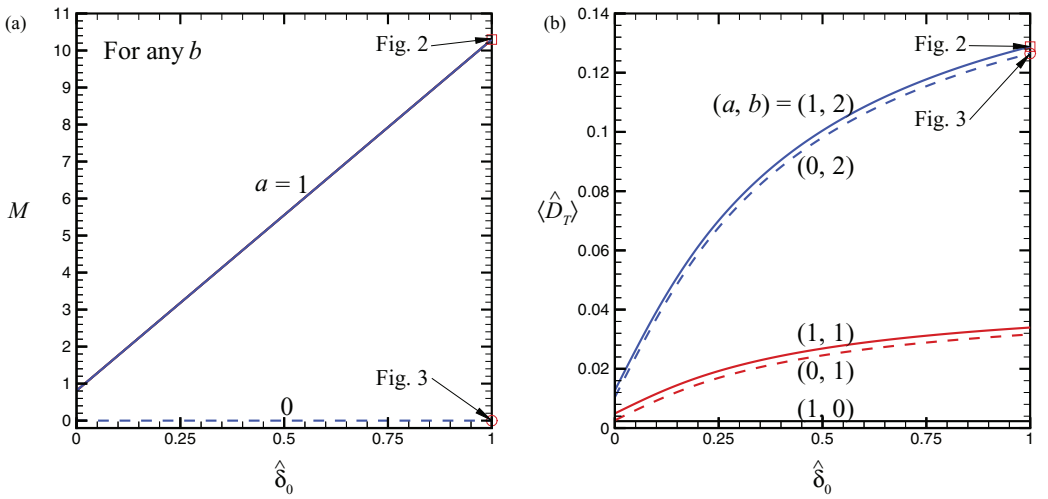

FIG. 1. For uniform slip ($\sigma = 0$) and $\hat{\kappa} = 10$, (a) the mobility M and (b) the averaged dispersion coefficient $\langle \hat{D}_T \rangle$, as functions of the slip length $\hat{\delta}_0$, where the solid and dashed lines are for $a = 1$ and $a = 0$, respectively. See Figs. 2 and 3 for the cases marked with a symbol.

For a sinusoidal slip length distribution $\hat{\delta}(\hat{z})$ given above, the effective hydrodynamic slip length can be deduced from Eqs. (9) and (21) as follows:

$$\hat{\delta}_{\text{eff}} = \frac{1}{4}\left(\sqrt{1 + 8\hat{\delta}_0} - 1\right) \qquad \text{for } \sigma = 1. \tag{41}$$

In practice, the slip length and the potential distributions are independent of each other. Therefore, there can be an arbitrary phase shift between the two distributions when they are both periodically modulated. However, for the sake of simplicity, we only consider two particular cases of phase shift in our discussion here: in-phase when b is positive, and half-period out-of-phase when b is negative.

A. Uniform slip

We first consider the case when the slip length is uniformly distributed, i.e., $\sigma = 0$ and $\hat{\delta} = \hat{\delta}_0$. For this particular case, the EO mobility, as already given in Eq. (22), is

$$M = a\left[1 + \left(\hat{\kappa}\hat{\delta}_0 - \frac{2}{\hat{\kappa}}\right)\frac{I_1(\hat{\kappa})}{I_0(\hat{\kappa})}\right]. \tag{42}$$

Hence, the section-mean velocity is affected by the steady component, a, but not the amplitude of the modulation component, b, of the wall potential. It also increases linearly with the slip length $\hat{\delta}_0$. The dependence of M on a and $\hat{\delta}_0$ is illustrated in Fig. 1(a).

While M is independent of b, the dispersion coefficient is in sharp contrast much affected by b, as can be seen in Fig. 1(b). Let us first examine the case $a = 1$ (solid lines). When $b = 0$, the wall potential is also uniformly distributed, for which $\hat{D}_T$ is given by Eq. (33). The dispersion coefficient is independent of slip, and is of order 10^{-3}, as already noted above. By introducing an alternating component to the wall potential, the average dispersion coefficient $\langle \hat{D}_T \rangle$ can be significantly enhanced by one or two orders of magnitude for sufficiently large slip. Increasing the amplitude of the alternating component of $\hat{\zeta}$ will have no effect on the section-mean flow, but can appreciably enhance the local dispersion coefficient. Let us then examine the case $a = 0$ (dashed lines), for which the section-mean flow vanishes. Despite the vanishing of the mean flow, the dispersion coefficient is similarly enhanced by the introduction of an alternating modulation component to the wall potential; it has nearly the same value as that for the same b in the case of $a = 1$. In summary, for a uniform slip distribution, the EO mobility M is affected only by the mean

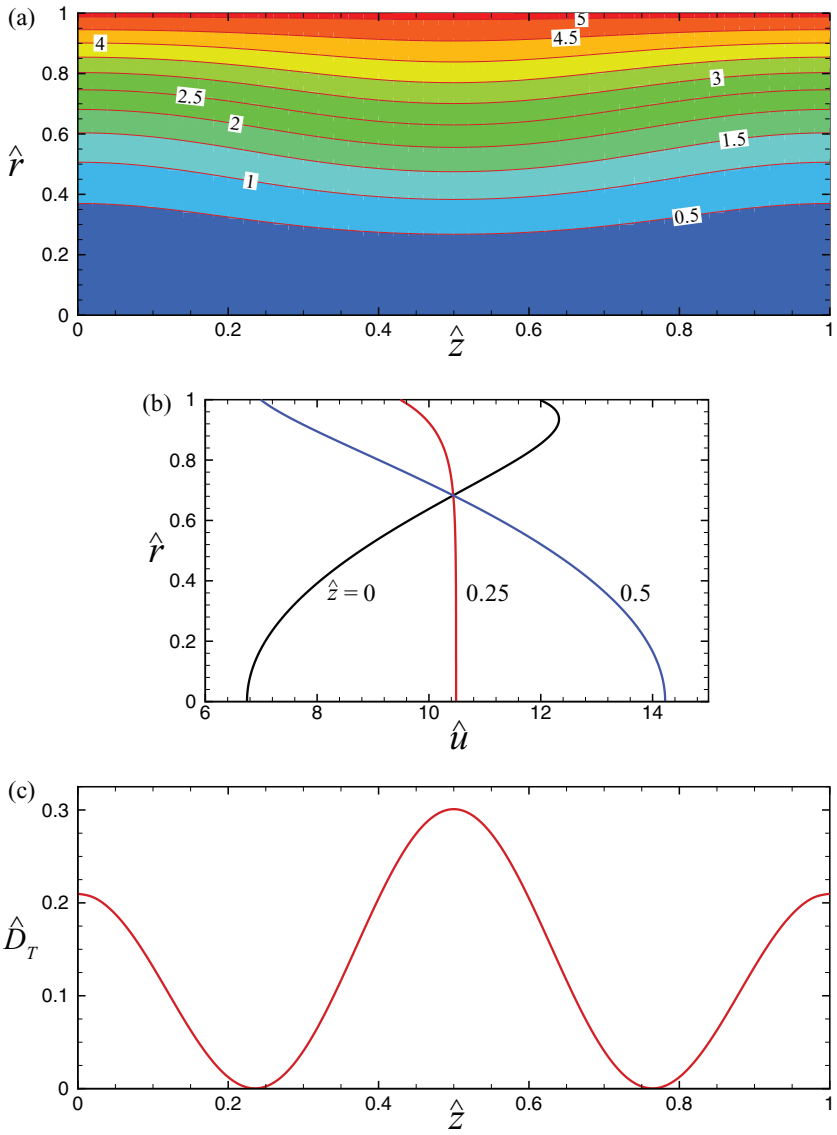

FIG. 2. For the case of uniform slip ($\sigma = 0$, $\hat{\delta}_0 = 1$), alternating wall potential of non-zero mean ($a = 1$, $b = 2$) and $\hat{\kappa} = 10$, (a) contours of the streamfunction $\Psi(\hat{r}, \hat{z})$, (b) velocity profiles $\hat{u}(\hat{r})$ at $\hat{z} = 0$, 0.25, 0.5, and (c) axial distribution of the dispersion coefficient $\hat{D}_T(\hat{z})$.

wall potential a, while the average dispersion coefficient $\langle \hat{D}_T \rangle$ is much affected by the amplitude, b, of the alternating component of the wall potential. One can choose suitable values of a, b, and $\hat{\delta}_0$ to achieve different scenarios of flow and transport (e.g., flow with little mixing, or zero net flow with mixing, and so on).

We illustrate in Figs. 2 and 3 the flow field and the axial distribution of the dispersion coefficient for two particular cases, which for easy reference are marked with symbols in Fig. 1. The velocity profile $\hat{u}(\hat{r}, \hat{z})$ and the streamfunction $\Psi(\hat{r}, \hat{z})$ are calculated by Eqs. (18) and (20), respectively. Figure 2 is for the case $(a, b) = (1, 2)$, while Fig. 3 is for the case $(a, b) = (0, 2)$, where $\hat{\delta}_0 = 1$ and $\sigma = 0$ in both cases. To understand the flow pattern, we need to recall the two components that contribute to the flow: one directly due to the applied electric field, and one driven by the induced pressure gradient. The electrically driven flow has an almost plug-like velocity profile for large $\hat{\kappa}$, giving rise to very small dispersion. The indirect, pressure-driven flow has a parabolic velocity profile, which may give rise to much larger dispersion. The pressure gradient is induced so as to

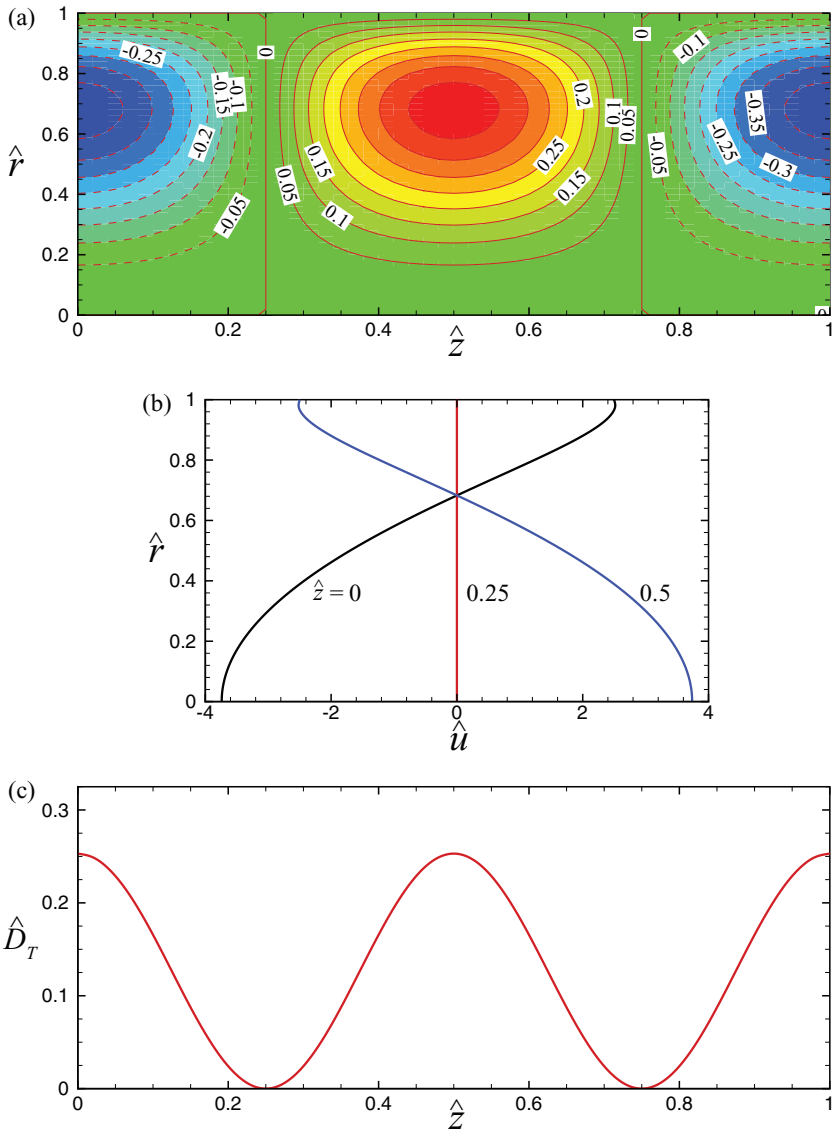

FIG. 3. For the case of uniform slip ($\sigma = 0$, $\hat{\delta}_0 = 1$), alternating wall potential of zero mean ($a = 0$, $b = 2$) and $\hat{\kappa} = 10$, (a) contours of the streamfunction $\Psi(\hat{r}, \hat{z})$, (b) velocity profiles $\hat{u}(\hat{r})$ at $\hat{z} = 0$, 0.25, 0.5, and (c) axial distribution of the dispersion coefficient $\hat{D}_T(\hat{z})$.

satisfy the continuity of flow. At places where the wall potential or slip is stronger than the system average, an adverse pressure gradient is induced, causing a backward flow to counterbalance the otherwise stronger EO flow. At places where the wall potential or slip is weaker than the average, a favorable pressure gradient is induced, causing a forward flow to supplement the otherwise weaker EO flow. This explains why the velocity profile has an inverted parabolic shape (minimum at the center and maximum near the wall) at $\hat{z} = 0$, where the wall potential is the maximum positive, but has a nearly parabolic shape (maximum at the center and minimum near the wall) at $\hat{z} = 0.5$, where the potential is the maximum negative. Such complementary nature of flow profiles has been observed experimentally by Herr *et al.*[12] At the mid-point, $\hat{z} = 0.25$, the pressure gradient is zero, and therefore the profile is purely that of the EO flow. As a result, the velocity shear, and hence the dispersion coefficient, is locally the largest at $\hat{z} = 0$ and $\hat{z} = 0.5$, and is the smallest near $\hat{z} = 0.25$. The flow shown in Fig. 2(a) is forward in direction everywhere, mainly because of a sufficiently large mean wall potential, $a = 1$. The flow is forward even near $\hat{z} = 0.5$ where the wall potential

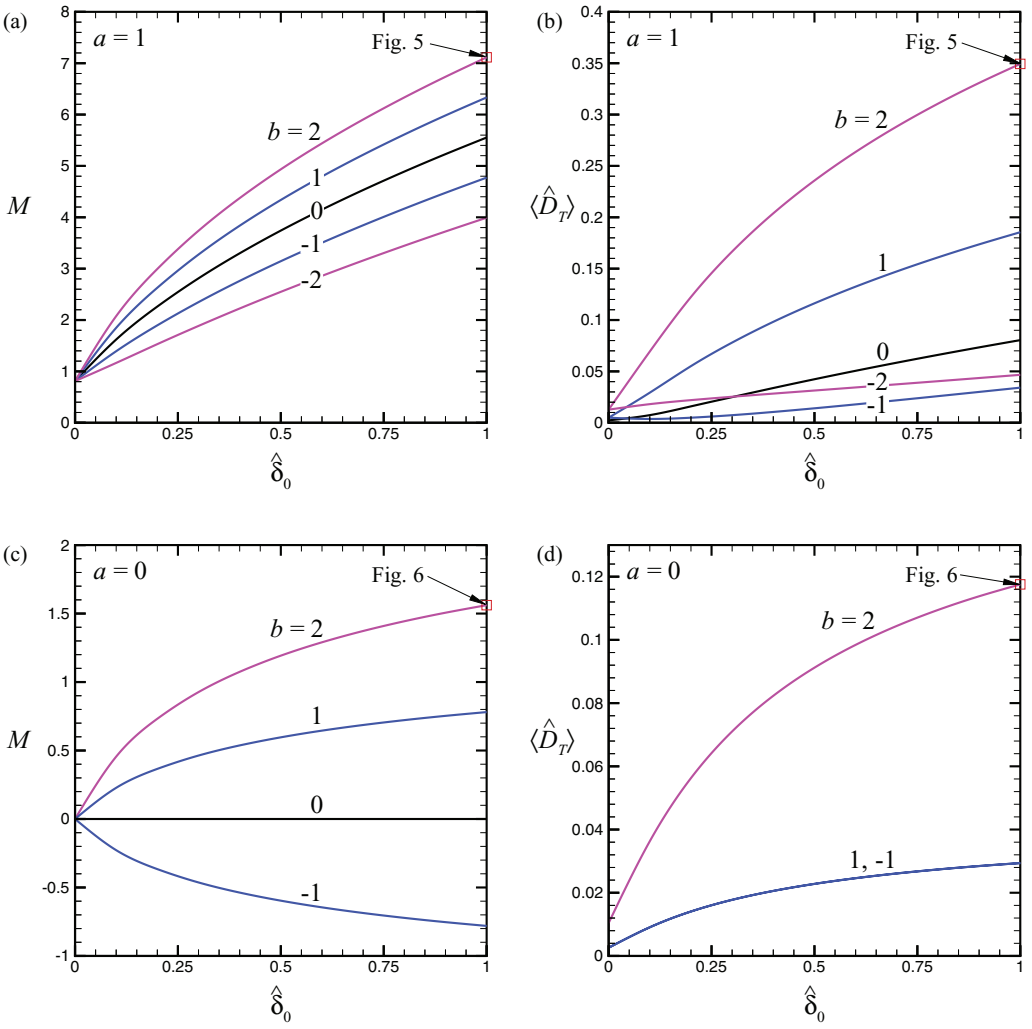

FIG. 4. For non-uniform slip ($\sigma = 1$) and $\hat{\kappa} = 10$, (a) and (c) the mobility M, and (b) and (d) the averaged dispersion coefficient $\langle \hat{D}_T \rangle$, as functions of the slip length $\hat{\delta}_0$, where $a = 1$ in (a) and (b) and $a = 0$ in (c) and (d). See Figs. 5 and 6 for the cases marked with a symbol.

is of an opposite sign. When the mean wall potential vanishes, $a = 0$, the flow becomes purely recirculatory with zero net discharge, as shown in Fig. 3(a).

B. Non-uniform slip

We next consider the case when the slip length is non-uniformly distributed, i.e., $\sigma = 1$. The slip length has the peak value of $2\hat{\delta}_0$ at $\hat{z} = n$, and has the minimum value of zero at $\hat{z} = n + 1/2$, where $n = 0, 1, 2, \ldots$. Results are shown in Fig. 4.

A non-uniform slip distribution may bring forth effects dramatically different from those by a uniform slip distribution. First, the EO mobility M will be affected by both a and b, the mean as well as the alternating components of the wall potential. Also, the enhancement of $\langle \hat{D}_T \rangle$ due to the alternating component of the wall potential can be appreciably amplified when subject to a non-uniform slip distribution. On comparing Figs. 1(a), 1(b), 4(a), and 4(b), one finds that a non-uniform slip distribution interacting with a non-uniform wall potential distribution may give rise to results different from those when the distributions are each uniform and equal to the mean of the corresponding non-uniform distributions. For $(a, b) = (1, 1)$ and $\hat{\delta}_0 = 1$ as an example, the

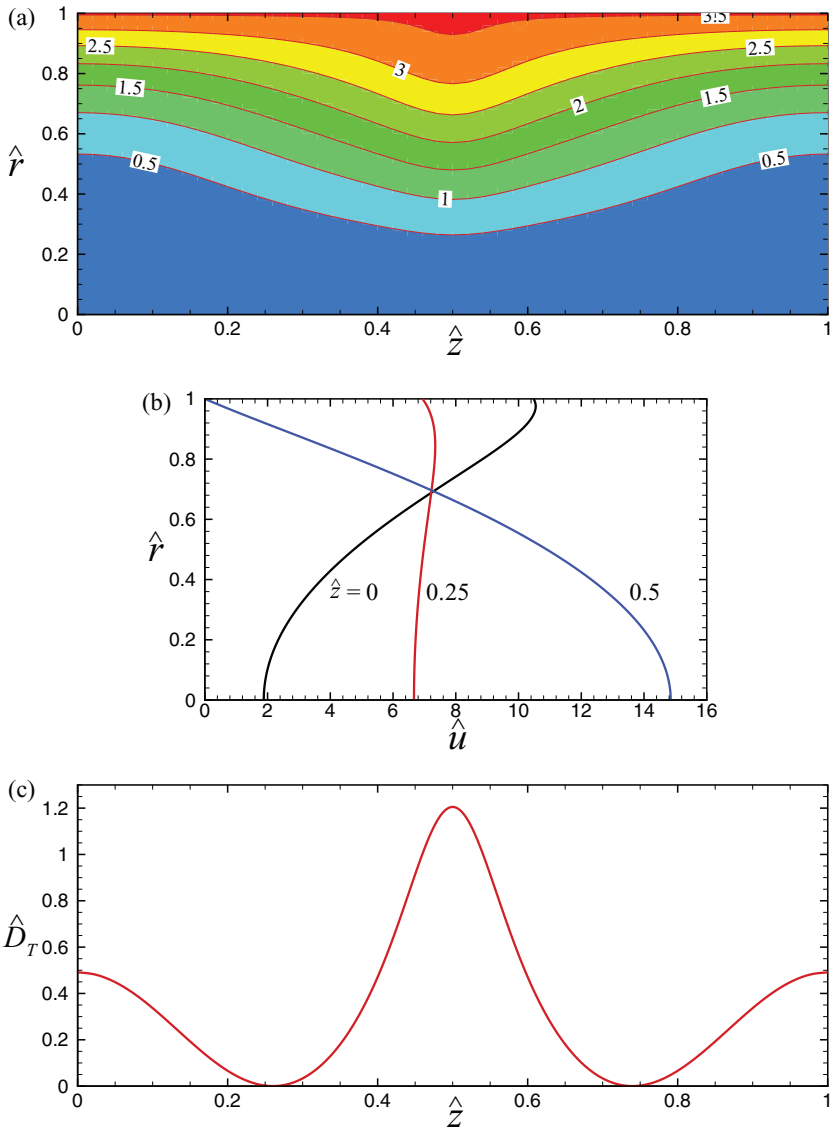

FIG. 5. For the case of non-uniform slip ($\sigma = 1$, $\hat{\delta}_0 = 1$), alternating wall potential of non-zero mean ($a = 1$, $b = 2$) and $\hat{\kappa} = 10$, (a) contours of the streamfunction $\Psi(\hat{r}, \hat{z})$, (b) velocity profiles $\hat{u}(\hat{r})$ at $\hat{z} = 0,\ 0.25,\ 0.5$, and (c) axial distribution of the dispersion coefficient $\hat{D}_T(\hat{z})$.

mobility is smaller, but the average dispersion coefficient is larger, when the slip is non-uniformly distributed than when it is uniformly distributed. For given non-uniform distributions for the slip and wall potential where $a > 0$, the mobility and the average dispersion coefficient are the largest when the two distributions are in phase (i.e., the peak slip meets the highest potential while the no-slip meets the lowest potential), and are the smallest when the distributions are completely out of phase (i.e., the peak slip meets the lowest potential while the no-slip meets the highest potential). This is true even if the lowest potential is of an opposite sign to the highest potential when $|b| > a > 0$.

Recall that in the case of uniform slip, no net flow can occur when $a = 0$ for any b. Here, we see that, as shown in Fig. 4(c), net EO flow can happen when the mean wall potential is zero, $a = 0$, as long as the alternating wall potential is non-zero, $b \neq 0$, and the slip is non-uniformly distributed. The fact that an electro-neutral surface may give rise to large EO flow, when under the effect of non-uniform hydrodynamic slip, has been pointed out by Belyaev and Vinogradova.[25] Increasing b will increase not only the flow, but also the average dispersion coefficient, as shown in Fig. 4(d).

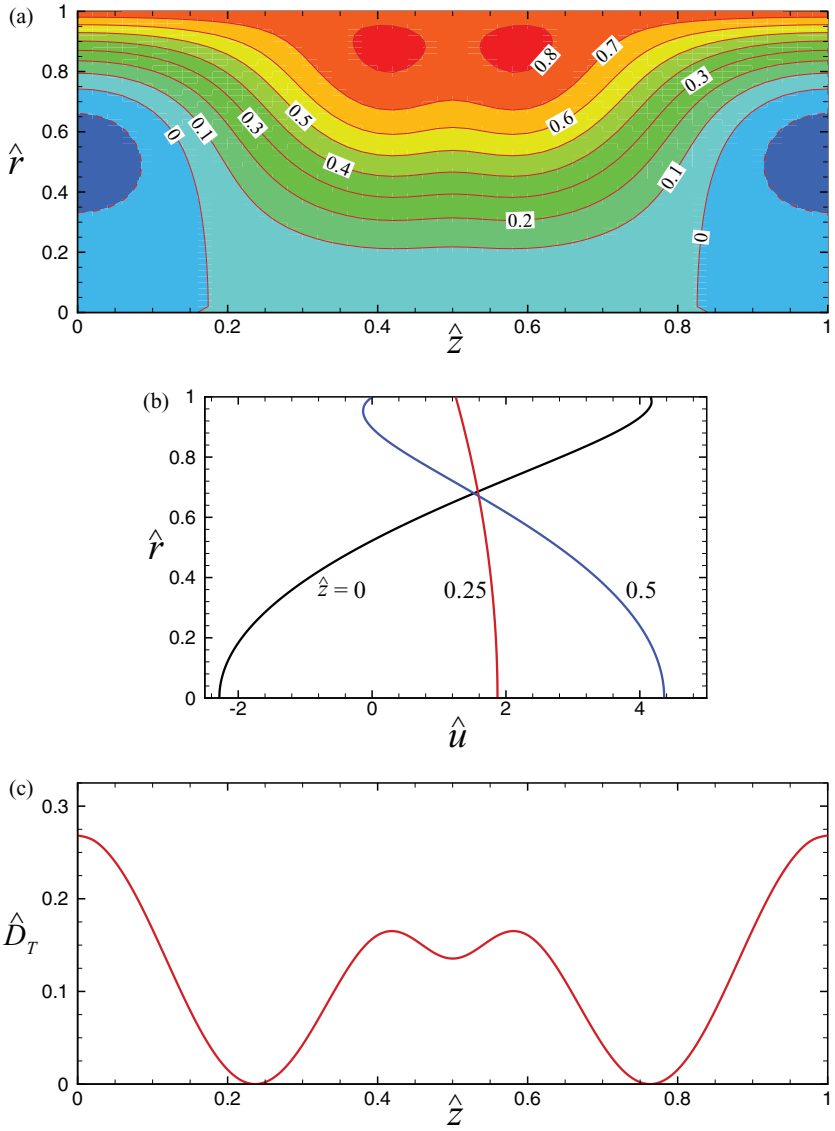

FIG. 6. For the case of non-uniform slip ($\sigma = 1, \hat{\delta}_0 = 1$), alternating wall potential of zero mean ($a = 0, b = 2$) and $\hat{\kappa} = 10$, (a) contours of the streamfunction $\Psi(\hat{r}, \hat{z})$, (b) velocity profiles $\hat{u}(\hat{r})$ at $\hat{z} = 0$, 0.25, 0.5, and (c) axial distribution of the dispersion coefficient $\hat{D}_T(\hat{z})$.

Negating the value of b will reverse the flow direction, but will not alter the dispersion coefficient. We further find that when $a = 0$, varying the phase between the slip and wall potential distributions will have effect only on the mobility (for its sign and magnitude), but not on the average dispersion coefficient $\langle \hat{D}_T \rangle$.

We then illustrate in Figs. 5 and 6 the flow field and the axial distribution of the dispersion coefficient for two particular cases, which for easy reference are marked with symbols in Fig. 4. Figure 5 is for the case $(a, b) = (1, 2)$, while Fig. 6 is for the case $(a, b) = (0, 2)$, where $\hat{\delta}_0 = 1$ and $\sigma = 1$ in both cases. These two cases can be compared with those shown in Figs. 2 and 3, bearing in mind that the slip is non-uniformly distributed in the former, but is uniformly distributed in the latter. For the case shown in Fig. 5, the maximum slip ($\hat{\delta} = 2$) meets the positive peak wall potential ($\hat{\zeta} = 3$) at $\hat{z} = 0$, while the zero slip meets the negative peak wall potential ($\hat{\zeta} = -1$) at $\hat{z} = 0.5$. Enhanced by the non-uniform slip, the contrast in the EO forcing between these two sections is larger than that in the uniform-slip case. Consequently, a larger pressure gradient is induced to force

flow through the section of the highest resistance, resulting in a much stronger velocity gradient and, hence, dispersion coefficient at $\hat{z} = 0.5$. The case shown in Fig. 6 corresponds to an electro-neutral wall (i.e., zero average charge). The net flow is forward in this case, because the positive potential, which is associated with the higher slip of the wall, will dominate. The forward flow encounters resistance, thereby forming recirculation cells, near the region of negative wall potential. The flow is convergent and confined to the central part of the channel on passing between two such recirculation rolls. The flow then spreads out to become an annular stream enclosing a central recirculation zone on passing through the region of positive wall potential. This kind of successive convergent and divergent flow is also conducive to mixing. Owing to a larger zone of recirculatory flow near $\hat{z} = 0$, the dispersion in this case is stronger at $\hat{z} = 0$ than at $\hat{z} = 0.5$.

V. CONCLUDING REMARKS

Using the lubrication approximation, we have analytically deduced the mobility and the dispersion coefficient for steady EO flow through a circular channel under the combined effect of charge and hydrodynamic slip modulation on the wall of the channel. The wall potential and the slip length are assumed to vary slowly and periodically in the axial direction. We have shown that a variety of scenarios corresponding to different degrees of flow and dispersion can be achieved by controlling the slip and wall potential distributions. For given mean values for the slip and the wall potential, the mobility is the largest and the dispersion is the weakest when both slip and wall potential are uniformly distributed (i.e., homogeneous wall). For an alternating wall potential distribution with a zero mean interacting with uniform slip, the mobility is always zero, but the dispersion can be locally large when both the amplitude of the wall potential distribution and the slip are sufficiently large. When the slip and the wall potential are both non-uniformly distributed, their interaction can give rise to effect very different from that when they are uniformly distributed and equal to the mean values of the non-uniform distributions. When their mean values are non-zero, the maximum possible dispersion effect happens when the two distributions are in phase, i.e., when the maximum slip is superposed to the highest wall potential and the minimum slip is superposed to the lowest wall potential. We have also explained that the dispersion coefficient is locally affected by the axial pressure gradient that is induced to maintain the continuity of flow. The pressure gradient gives rise to a parabolic velocity profile, which in general has stronger shear, thereby leading to larger dispersion, than the nearly plug-like velocity profile of EO flow. The presence of slip, whether uniformly or non-uniformly distributed, can significantly amplify the increased dispersion caused by induced pressure gradient brought about by the non-uniformity of wall potential.

ACKNOWLEDGMENTS

The work was financially supported by the Research Grants Council of the Hong Kong Special Administrative Region, China, through Project Nos. HKU 715609E and HKU 715510E.

[1] S. Datta and S. Ghosal, "Characterizing dispersion in microfluidic channels," Lab Chip **9**, 2537 (2009).
[2] M. Martin and G. Guiochon, "Axial dispersion in open-tubular capillary liquid chromatography with electroosmotic flow," Anal. Chem. **56**, 614 (1984).
[3] R. Datta and V. R. Kotamarthi, "Electrokinetic dispersion in capillary electrophoresis," AIChE J. **36**, 916 (1990).
[4] S. K. Griffiths and R. H. Nilson, "Hydrodynamic dispersion of a neutral nonreacting solute in electroosmotic flow," Anal. Chem. **71**, 5522 (1999).
[5] S. K. Griffiths and R. H. Nilson, "Electroosmotic fluid motion and late-time solute transport for large zeta potentials," Anal. Chem. **72**, 4767 (2000).
[6] E. K. Zholkovskij, J. H. Masliyah, and J. Czarnecki, "Electroosmotic dispersion in microchannels with a thin double layer," Anal. Chem. **75**, 901 (2003).
[7] E. K. Zholkovskij and J. H. Masliyah, "Hydrodynamic dispersion due to combined pressure-driven and electroosmotic flow through microchannels with a thin double layer," Anal. Chem. **76**, 2708 (2004).
[8] A. D. Stroock and G. M. Whitesides, "Controlling flows in microchannels with patterned surface charge and topography," Acc. Chem. Res. **36**, 597 (2003).
[9] H. Zhao and H. H. Bau, "Effect of secondary flows on Taylor–Aris dispersion," Anal. Chem. **79**, 7792 (2007).
[10] B. Potoček, B. Gaš, E. Kenndler, and M. Štědrý, "Electroosmosis in capillary zone electrophoresis with non-uniform zeta potential," J. Chromatogr. A **709**, 51 (1995).

[11] D. Long, H. A. Stone, and A. Ajdari, "Electroosmotic flows created by surface defects in capillary electrophoresis," J. Colloid Interface Sci. **212**, 338 (1999).
[12] A. E. Herr, J. I. Molho, J. G. Santiago, M. G. Mungal, and T. W. Kenny, "Electroosmotic capillary flow with nonuniform zeta potential," Anal. Chem. **72**, 1053 (2000).
[13] S. Ghosal, "Band broadening in a microcapillary with a stepwise change in the ζ-potential," Anal. Chem. **74**, 4198 (2002).
[14] J. K. Towns and F. E. Regnier, "Impact of polycation adsorption on efficiency and electroosmotically driven transport in capillary electrophoresis," Anal. Chem. **64**, 2473 (1992).
[15] S. Ghosal, "The effect of wall interactions in capillary-zone electrophoresis," J. Fluid Mech. **491**, 285 (2003).
[16] E. K. Zholkovskij, A. E. Yaroshchuk, J. H. Masliyah, and J. P. Ribas, "Broadening of neutral solute band in electroosmotic flow through submicron channel with longitudinal non-uniformity of zeta potential," Colloids Surf., A **354**, 338 (2010).
[17] V. M. Muller, I. P. Sergeeva, V. D. Sobolev, and N. V. Churaev, "Boundary effects in the theory of electrokinetic phenomena," Colloid J. USSR **48**, 606 (1986).
[18] N. V. Churaev, J. Ralston, I. P. Sergeeva, and V. D. Sobolev, "Electrokinetic properties of methylated quartz capillaries," Adv. Colloid Interface Sci. **96**, 265 (2002).
[19] L. Joly, C. Ybert, E. Trizac, and L. Bocquet, "Hydrodynamics within the electric double layer on slipping surfaces," Phys. Rev. Lett. **93**, 257805 (2004).
[20] A. Ajdari and L. Bocquet, "Giant amplification of interfacially driven transport by hydrodynamic slip: Diffusio-osmosis and beyond," Phys. Rev. Lett. **96**, 186102 (2006).
[21] T. M. Squires, "Electrokinetic flows over inhomogeneously slipping surfaces," Phys. Fluids **20**, 092105 (2008).
[22] S. S. Bahga, O. I. Vinogradova, and M. Z. Bazant, "Anisotropic electro-osmotic flow over super-hydrophobic surfaces," J. Fluid Mech. **644**, 245 (2010).
[23] H. Zhao, "Streaming potential generated by a pressure-driven flow over superhydrophobic stripes," Phys. Fluids **23**, 022003 (2011).
[24] O. I. Vinogradova and A. V. Belyaev, "Wetting, roughness and flow boundary conditions," J. Phys.: Condens. Matter **23**, 184104 (2011).
[25] A. V. Belyaev and O. I. Vinogradova, "Electro-osmosis on anisotropic superhydrophobic surfaces," Phys. Rev. Lett. **107**, 098301 (2011).
[26] C. O. Ng and H. C. W. Chu, "Electrokinetic flows through a parallel-plate channel with slipping stripes on walls," Phys. Fluids **23**, 102002 (2011).
[27] A. Ajdari, "Generation of transverse fluid currents and forces by an electric field: Electro-osmosis on charge-modulated and undulated surfaces," Phys. Rev. E **53**, 4996 (1996).
[28] A. Ajdari, "Transverse electrokinetic and microfluidic effects in micropatterned channels: Lubrication analysis for slab geometries," Phys. Rev. E **65**, 016301 (2001).
[29] S. Ghosal, "Lubrication theory for electro-osmotic flow in a microfluidic channel of slowly varying cross-section and wall charge," J. Fluid Mech. **459**, 103 (2002).
[30] C. O. Ng and Q. Zhou, "Electro-osmotic flow through a thin channel with gradually varying wall potential and hydrodynamic slippage," Fluid Dyn. Res. **44**, 055507 (2012).
[31] W. M. Deen, *Analysis of Transport Phenomena*, 2nd ed. (Oxford University Press, Oxford, 2012).
[32] C. L. Rice and R. Whitehead, "Electrokinetic flow in a narrow cylindrical capillary," J. Phys. Chem. **69**, 4017 (1965).
[33] J. Yang and D. Y. Kwok, "Analytical treatment of flow in infinitely extended circular microchannels and the effect of slippage to increase flow efficiency," J. Micromech. Microeng. **13**, 115 (2003).
[34] H. C. W. Chu and C. O. Ng, "Oscillatory electroosmotic flow through a channel with slipping stripes on walls," in *Proceedings of the 23rd International Congress on Theoretical and Applied Mechanics, Beijing, China*, 19–24 August 2012.
[35] C. C. Mei, J. L. Auriault, and C. O. Ng, "Some applications of the homogenization theory," Adv. Appl. Mech. **32**, 277 (1996).
[36] C. O. Ng, "Dispersion in steady and oscillatory flows through a tube with reversible and irreversible wall reactions," Proc. R. Soc. A **462**, 481 (2006).
[37] C. O. Ng, "How does wall slippage affect hydrodynamic dispersion?" Microfluid. Nanofluid. **10**, 47 (2011).